2020 54th Asilomar Conference on Signals, Systems, and Computers | 978-0-7381-3126-9/20/$31.00 ©2020 IEEE | DOI: 10.1109/IEEECONF51394.2020.9443356

Limits of Transmit Beamforming for Massive MIMO Radar

Arindam Bose, Ahsan Ghauri, and Mojtaba Soltanalian
Department of Electrical and Computer Engineering, University of Illinois at Chicago, Chicago, IL 60607
Email: {abose4, ghauri1, msol}@uic.edu

***Abstract*—Massive MIMO has garnered a significant deal of interest recently. In this paper, we discuss the fundamental limitations of the resolution of beampatterns produced by MIMO radar when the number of antennas grows large—leading to a massive MIMO scenario in the context of radar. In particular, we examine whether any arbitrary beampattern can be formed as the number of antennas N increases, i.e., as $N \to \infty$. We further study the improvement of the resolution of beampattern shaping as N grows large. This is to see if the potential of massive MIMO can be unleashed in active sensing and beamforming applications.**

***Index Terms*—active sensing, beamforming, beampattern, massive MIMO, radar**

I. Introduction

In the last decades, multiple input multiple output (MIMO) technology has become an essential part of many active sensing systems, while its use has been extensively studied in the literature (see [1] and the references therein). The use of MIMO radars has enriched spectral diversity and improved spatial resolution of millimeter-wave (mmWave) and centimeter-wave (cmWave) radar systems due to its large array gains, even in lower signal-to-noise ratio (SNR) scenarios. Massive MIMO, is an extension of MIMO, that essentially groups together a large number of antennas (much more than the number of targets) at the transmitter (Tx) and receiver (Rx) to obtain better spectrum efficiency with improved power consumption in communication. Unlike the conventional MIMO systems, the number of antennas in the Tx and Rx of a massive MIMO radar can be from a few dozen to several hundreds, which represents a significant increase. This helps the radar station to project beams toward multiple targets simultaneously using the same time-frequency spectra.

The concept of massive MIMO for wireless communications was first introduced by Marzetta in his seminal paper [4]. Since then, the notion has found potential applications in many other areas including radar and beamforming [5]–[7]. The ability of massive MIMO to multiply the capacity of the antenna links and robustness to jamming has made it an essential element of wireless communication standards including 802.11n (Wi-Fi), 802.11ac (Wi-Fi), HSPA+, WiMAX and LTE [8].

Shaping beampatterns or beamforming is a critical task in MIMO systems where multiple antennas are used to control the direction of a electromagnetic wavefront by appropriately weighting the magnitude or phase of individual antenna signals in an array of the antennas, as well as designing the signals themselves [10]. In this paper, we seek to uncover the fundamental limits of the resolution of beamforming with respect to the number of antennas. We will examine, as the number of antennas, N, grows large,

- What beampatterns can be realized if the covariance matrix of the transmit signals may be chosen at will?
- How rapidly we can change the beampattern for closely located angles? and
- How our ability to form a peak in a beampattern is governed by the number of antennas?

Notation: We use bold-lowercase and bold-uppercase letters to represent vectors and matrices, respectively. x_i denotes the i-th element of the vector $\boldsymbol{x}$. The superscripts $(\cdot)^*$, $(\cdot)^T$, and $(\cdot)^H$ represent the conjugate, the transpose, and the Hermitian operators, respectively. $\boldsymbol{X} \succeq \boldsymbol{Y}$ is equivalent with $\boldsymbol{X}-\boldsymbol{Y}$ being positive semidefinite (p.s.d.). The set of complex matrices are denoted by $\mathbb{C}$.

II. Problem Formulation

Consider an array of N transmit antennas with $x_n(l) \in \mathbb{C}$ being the l^{th} sample of the discrete-time base-band signal transmitted by the n^{th} antenna. Let θ denote the location of a generic point in space, for example, its azimuth angle and range. Then, under the assumption that the transmitted probing signals are narrow-band and that the propagation is nondispersive, the base-band signal at the point of interest (PoI) can be described by the expression (see, e.g. [12])

$$\sum_{n=1}^{N} e^{-j2\pi f_0 \tau_n(\theta)} x_n(l) \triangleq \boldsymbol{a}^H(\theta)\boldsymbol{x}(l), \quad l \in \{1, 2, \cdots, L\} \tag{1}$$

where f_0 is the carrier frequency of the array, $\tau_n(\theta)$ is the time needed by the signal emitted via the n^{th} antenna to arrive at the PoI, and L denotes the number of samples of each transmitted signal pulse,

$$\boldsymbol{x}(l) = [x_1(l)\ x_2(l)\ \cdots\ x_N(l)]^T \tag{2}$$

and the *steering vector*,

$$\boldsymbol{a}(\theta) = [a_1(\theta)\ a_2(\theta)\ \cdots\ a_N(\theta)]^T, \tag{3}$$

is defined in such a way that $a_n(\theta) = e^{j2\pi f_0 \tau_n(\theta)}$. Assuming the transmit array of the radar is calibrated, $\boldsymbol{a}(\theta)$ is a known function of θ. It follows from (1) that the power of the probing signal at a generic focal point with location θ is given by

$$p(\theta) = \boldsymbol{a}^H(\theta)\boldsymbol{R}\boldsymbol{a}(\theta), \tag{4}$$

where $\boldsymbol{R}$ is the covariance matrix of $\boldsymbol{x}(l)$, *i.e.*,

$$\boldsymbol{R} = \mathbb{E}\left\{\boldsymbol{x}(l)\boldsymbol{x}^H(l)\right\}. \tag{5}$$

The above spatial spectrum is called the *transmit beampattern*. Herein, we assume that the MIMO system employs a uniform linear array (ULA) where the signal traversal time can simply be approximated as $\tau_n(\theta) = n\theta$. Hence each element of the steering vector reduces to $a_n(\theta) = e^{jn\xi\theta}$, where $\xi = 2\pi f_0$. Furthermore, by normalizing ξ to 1, the transmit beampattern at a generic θ can be simplified as

$$p(\theta) = \sum_{k=1}^{N}\sum_{l=1}^{N} R_{k,l} e^{j(k-l)\theta}, \tag{6}$$

where $R_{k,l} = [\boldsymbol{R}]_{k,l}$.

III. Limits of Beamforming

A. Realization and Resolution

Note that a covariance matrix $\boldsymbol{R}$ of size $N \times N$, can always be realized with N independent streams of signals, transmitted by N antennas. In this subsection, the question we aim to answer is the following:

What functions $p(\theta)$ can be realized using N antennas, if the covariance matrix $\boldsymbol{R} \in \mathbb{C}^{N\times N}$ may be chosen at will?

Definition 1. The *Zero-Order Resolution*, $I_0(N)$ is defined as the number of points in space for which we can exactly determine the power, *i.e.*, we can design the covariance matrix of the signal transmitted by N antennas in order to achieve the allocated power.

Note that an $N \times N$ Hermitian matrix $\boldsymbol{R}$ has, in itself, N^2 real-valued variables. As a result, even without considering the positive semi-definiteness constraint, $\boldsymbol{R}$ may be uniquely identified by fixing the value of $p(\theta)$ at N^2 points. The matrix $\boldsymbol{R}$ can then be determined by solving a linear system of equations. This shows that, for a limited number of antennas, one will have difficulty producing beampatterns of interest that are very complex. What remains is to see if such complex beampatterns can be realized if $N \to \infty$. In other words, we seek to see if we can construct $\boldsymbol{R}$ of *arbitrary size* that will realize a given $p(\theta)$. To address this problem, we further investigate whether a certain zero-order resolution can be guaranteed for a given number of antennas, and then extend our investigation to the large-scale scenario.

— *The Finite-Energy Case:* In the following we first consider the finite energy case *i.e.*, when the growth of $\boldsymbol{R}$ (or more precisely its Frobenius norm) is bounded by a finite scalar, guaranteeing the construction of a given resolution proves to be difficult. Note that

$$p(\theta) = \boldsymbol{a}^H(\theta)\boldsymbol{R}\boldsymbol{a}(\theta) = \operatorname{tr}\left(\boldsymbol{R}\boldsymbol{a}(\theta)\boldsymbol{a}^H(\theta)\right) = \operatorname{tr}\left(\boldsymbol{R}\bar{\boldsymbol{A}}(\theta)\right), \tag{7}$$

where $\bar{\boldsymbol{A}}(\theta) = \boldsymbol{a}(\theta)\boldsymbol{a}^H(\theta)$. Let $\boldsymbol{E} = \bar{\boldsymbol{A}}(\theta_2) - \bar{\boldsymbol{A}}(\theta_1)$ for two arbitrary points θ_1 and θ_2. Hence,

$$|p(\theta_2) - p(\theta_1)| = |\operatorname{tr}(\boldsymbol{R}\boldsymbol{E})| \tag{8}$$

which will be small for a small $|\theta_2 - \theta_1|$. On the other hand, given the *smoothness* of $p(\theta)$, an N^2 point realization of the beampattern is achievable. To see how, consider the points of interest $\{\boldsymbol{a}(\theta_k)\}_{k=1}^{N^2}$ and their corresponding beam powers $\{\gamma_k\}_{k=1}^{N^2}$. Using the linear system described earlier, a Hermitian matrix $\boldsymbol{R}$ can be constructed that yields the desired power values at PoIs. However, this may violate the p.s.d. constraint on $\boldsymbol{R}$. In order to enforce the p.s.d. constraint, one may employ a diagonal loading of $\boldsymbol{R}$; *i.e.*, replacing $\boldsymbol{R}$ with $\boldsymbol{R} + (\lambda/N)\boldsymbol{I}$, which effectively produces the power $\{\gamma_k + \lambda\}_{k=1}^{N^2}$ at the PoIs. Note that adding $\lambda > -\min\{\operatorname{eig}(\boldsymbol{R})\}$ to $\{\gamma_k\}_{k=1}^{N^2}$ only smoothens the desired beam pattern, making the beampattern attainable. This is connected to the *Rate of Innovation* metric discussed in Section III-B.

— *The Unconstrained-Energy Case:* In such a scenario, the p.s.d. constraint on $\boldsymbol{R}$ can be equivalently expressed as the existence of a square matrix, $\boldsymbol{X} \in \mathbb{C}^{N\times N}$ such that $\boldsymbol{R} = \boldsymbol{X}^H\boldsymbol{X}$. Accordingly, the beampattern matching constraint $p(\theta) = \boldsymbol{a}^H(\theta)\boldsymbol{R}\boldsymbol{a}(\theta)$ can be rewritten as

$$\|\boldsymbol{X}\boldsymbol{a}(\theta)\|_2 = \sqrt{p(\theta)}. \tag{9}$$

Suppose that the beam pattern $p(\theta)$ is to be realized at N locations $\{\theta_1, \theta_2, \cdots, \theta_K\}$. Satisfying (9) for all $\{\theta_k\}$ implies that there should exist unit-norm vectors $\{\boldsymbol{u}_k\}$ such that

$$\boldsymbol{X}\boldsymbol{a}(\theta_k) = \sqrt{p(\theta_k)}\,\boldsymbol{u}_k \tag{10}$$

for all $k \in \{1, 2, \cdots, N\}$. Let

$$\begin{aligned} \boldsymbol{A} &= [\boldsymbol{a}(\theta_1)\ \boldsymbol{a}(\theta_2)\ \cdots\ \boldsymbol{a}(\theta_N)], \\ \boldsymbol{U} &= [\boldsymbol{u}_1\ \boldsymbol{u}_2\ \cdots\ \boldsymbol{u}_N], \\ \boldsymbol{D} &= \operatorname{Diag}\left(\left[\sqrt{p(\theta_1)}\ \sqrt{p(\theta_2)}\ \cdots\ \sqrt{p(\theta_N)}\right]\right). \end{aligned} \tag{11}$$

Noting that $\boldsymbol{A}$ is a non-singular Vandermonde matrix, one can obtain

$$\boldsymbol{X} = \boldsymbol{U}\boldsymbol{D}\boldsymbol{A}^{-1}, \tag{12}$$

or equivalently $\boldsymbol{R} = \boldsymbol{A}^{-H}\boldsymbol{D}\boldsymbol{U}^H\boldsymbol{U}\boldsymbol{D}\boldsymbol{A}^{-1}$. This implies that if the energy is not constrained, one can always achieve a zero-order resolution of N using above construction. Interestingly, there is a lot of freedom in forming a desirable covariance matrix, owing to the fact that $\boldsymbol{U}$ is a matrix with unit-norm columns that can be chosen rather arbitrarily. Furthermore, one can observe that if any subset of $\{\theta_k\}$ are close then $\boldsymbol{A}^{-1}$ will grow large, which in turn will lead to larger power in $\boldsymbol{R}$. Now, it would be interesting to see if this freedom can be exploited to fit the beampattern at more points and thus increase the zero-order resolution $I_0(N)$. In fact, it can be shown that this goal is not always achievable. To see why, we add a new point, say θ_{N+1}, to those already considered in (9):

$$\boldsymbol{X}\boldsymbol{a}(\theta_{N+1}) = \boldsymbol{U}\boldsymbol{D}\boldsymbol{A}^{-1}\boldsymbol{a}(\theta_{N+1}) = \sqrt{p(\theta_{N+1})}\,\boldsymbol{u}_{N+1}. \tag{13}$$

It is straightforward to verify that

$$\begin{aligned}\left\|\boldsymbol{U}\boldsymbol{D}\boldsymbol{A}^{-1}\boldsymbol{a}(\theta_{N+1})\right\|_2 &= \left\|\sum_{k=1}^{N}\left[\boldsymbol{D}\boldsymbol{A}^{-1}\boldsymbol{a}(\theta_{N+1})\right]_k \boldsymbol{u}_k\right\|_2 \\ &\leq \sum_{k=1}^{N}\left|\left[\boldsymbol{D}\boldsymbol{A}^{-1}\boldsymbol{a}(\theta_{N+1})\right]_k\right| \|\boldsymbol{u}_k\|_2 \\ &= \left\|\boldsymbol{D}\boldsymbol{A}^{-1}\boldsymbol{a}(\theta_{N+1})\right\|_1. \end{aligned} \tag{14}$$

As a result, the beampattern at θ_{N+1} may only be realized if

$$p(\theta_{N+1}) \leq \left\|\boldsymbol{D}\boldsymbol{A}^{-1}\boldsymbol{a}(\theta_{N+1})\right\|_1^2, \tag{15}$$

a condition which is not necessarily always met.

B. Rate of Innovation (I_1)

In this subsection, we will study the following:

How rapidly we can change the beampattern, $p(\theta)$ for closely located angles θ using N antennas?

Note that from (6),

$$\frac{\partial p(\theta)}{\partial \theta} = \sum_{k,l} j(k-l)R_{k,l}\, e^{j(k-l)\theta}, \tag{16}$$

which implies that

$$\left|\frac{\partial p(\theta)}{\partial \theta}\right| \leq 2\sum_{k>l}(k-l)\,|R_{k,l}| \triangleq I_1(\boldsymbol{R}) \tag{17}$$

It follows from the above that

$$|I_1(\boldsymbol{R})|^2 \leq 4 \underbrace{\left(\sum_{k>l}(k-l)^2\right)}_{(*)}\underbrace{\left(\sum_{k>l}|R_{k,l}|^2\right)}_{(\dagger)} \tag{18}$$

As to $(*)$,

$$\begin{aligned}\sum_{k>l}(k-l)^2 &= \sum_{k=1}^{N-1}(N-k)k^2 \\ &= \frac{N^2(N^2-1)}{12}.\end{aligned} \tag{19}$$

Moreover, $(\dagger)$ can be rewritten as

$$\sum_{k>l}|R_{k,l}|^2 = \frac{1}{2}\left(\|\boldsymbol{R}\|_F^2 - R_{\text{diag}}\right), \tag{20}$$

where $R_{\text{diag}} = \sum_k R_{k,k}^2$. Therefore,

$$|I_1(\boldsymbol{R})|^2 \leq \frac{1}{6}N^2(N^2-1)\left(\|\boldsymbol{R}\|_F^2 - R_{\text{diag}}\right). \tag{21}$$

Define

$$\alpha = \frac{\|\boldsymbol{R}\|_F^2 - R_{\text{diag}}}{\|\boldsymbol{R}\|_F^2}, \tag{22}$$

so that the following can be deduced:

$$\frac{|I_1(\boldsymbol{R})|^2}{\|\boldsymbol{R}\|_F^2} \leq \frac{\alpha}{6}N^2(N^2-1). \tag{23}$$

Note that α always appears in the interval $[0,1)$. While it is completely possible for α to become zero, especially when the signal $\boldsymbol{x}(l)$ has an *impulse-like autocorrelation*, the upper bound on α can be slightly improved. To see how, note that as $\boldsymbol{R}$ is p.s.d., any *sub-matrix* of it must be p.s.d. as well. For example, by choosing the 2×2 matrix formed by the intersections of k^{th} and l^{th} rows and columns respectively, the p.s.d. constraint dictates

$$R_{k,k}R_{l,l} \geq |R_{k,l}|^2, \tag{24}$$

for all k,l. As a result,

$$\begin{aligned}\left(\sum_{k=1}^{N}R_{k,k}\right)^2 &= \sum_{k=1}^{N}R_{k,k}^2 + \sum_{k\neq l}R_{k,k}R_{l,l} \\ &\geq \sum_{k=1}^{N}R_{k,k}^2 + \sum_{k\neq l}|R_{k,l}|^2 = \|\boldsymbol{R}\|_F^2.\end{aligned} \tag{25}$$

On the other hand, the Cauchy-Schwarz inequality implies that

$$\left(\sum_{k=1}^{N}R_{k,k}\right)^2 \leq N\left(\sum_{k=1}^{N}R_{k,k}^2\right) = N\,R_{\text{diag}} \tag{26}$$

It follows from (25) and (26) that

$$\frac{R_{\text{diag}}}{\|\boldsymbol{R}\|_F^2} \geq \frac{1}{N}, \tag{27}$$

or equivalently,

$$0 \leq \alpha \leq \frac{N-1}{N}. \tag{28}$$

More improvements can likely be accomplished by using larger sub-matrices, which remains out of the scope of this study. One interesting observation is that $\|\boldsymbol{R}\|_F^2$ in (23) can be replaced with a variable directly connected to the power of beampattern projected in the space. Our results can be summarized as the following theorem:

Theorem 1. *Assuming that the transmission power is fixed with respect to the number of antennas, N, the rate of innovation $I_1(N)$ behaves as $\mathcal{O}(N^2)$ with respect to N.*

C. Forming a Peak (I_2)

We study forming of a peak in the desired beampattern, or in other words, which is connected to the 2nd order resolution of beamforming. To form a peak one must be able to make the second derivative of $p(\theta)$ "large":

$$\frac{\partial^2 p(\theta)}{\partial \theta^2} = \sum_{k,l} -(k-l)^2 R_{k,l}\, e^{j(k-l)\theta} \tag{29}$$

which implies that

$$\left|\frac{\partial^2 p(\theta)}{\partial \theta^2}\right| \leq 2\sum_{k>l}(k-l)^2\,|R_{k,l}| \triangleq I_2(\boldsymbol{R}) \tag{30}$$

It follows that

$$|I_2(\boldsymbol{R})|^2 \leq 4 \underbrace{\left(\sum_{k>l}(k-l)^4\right)}_{(**)}\left(\sum_{k>l}|R_{k,l}|^2\right) \tag{31}$$

As to $(**)$,

$$\begin{aligned}\sum_{k>l}(k-l)^4 &= \sum_{k=1}^{N-1}(N-k)k^4 \\ &= \mathcal{O}(N^6).\end{aligned} \tag{32}$$

Consequently, by following similar arguments as in subsection III-B, the following theorem can be presented.

Theorem 2. *Assuming that the transmission power is fixed with respect to the number of antennas, N, forming of a peak in the beampattern, $I_2(N)$ behaves as $\mathcal{O}(N^3)$.*

IV. Numerical Studies

This section presents a numerical study of beampattern matching as the number of antennas N grows large. Our simulations closely follow the probing signal designing algorithm described in [14], where a transmit signal covariance matrix $\boldsymbol{R}$ of size $N \times N$ is synthesized in order to match, or rather approximate in a least square sense, a desired transmit beampattern, $d(\theta)$ with a zero-order resolution K. In [14], the authors consider choosing $\boldsymbol{R}$ under a uniform elemental constraint, *i.e.*,

$$R_{n,n} = c/N;$$

with given c. We adhere to this constraint for our simulations, as it is often encountered in real-world applications. Mathematically, the beampattern matching is accomplished by solving the following problem [14], [15]:

$$\begin{aligned}\min_{\zeta,\boldsymbol{R}} \ & \frac{1}{K}\sum_{k=1}^{K}\omega_k[\boldsymbol{a}^H(\theta_k)\boldsymbol{R}\boldsymbol{a}(\theta_k) - \zeta d(\theta_k)]^2 \\ \text{s.t.} \ & R_{n,n} = c/N, \ n = 1, \cdots, N, \\ & \boldsymbol{R} \succeq \boldsymbol{0},\end{aligned} \tag{33}$$

where $\zeta > 0$ is a scaling factor to be designed, and $\omega_k \geq 0$, $k \in \{1, \cdots, K\}$, is the emphasis weight allocated to the k^{th} grid point of the beampattern. In [15], the authors show that the above design problem can be formulated as a convex semidefinite quadratic problem (SQP) and can be solved efficiently in polynomial-time.

Our first series of numerical studies are presented in Fig. 1. In each experiment, we use different number of antennas in a ULA, and try to approximate a smooth sinusoidal beampattern (shown in *black*) that is defined for $[-90°, 90°]$ in the azimuth direction with $1°$ interval, *i.e.*, it consists of 181 points in 1D space. It can be easily seen in the Fig. 1(a) that as N increases, the desired beampattern can be realized more closely. The mean square errors (MSE) of approximation for different K is shown in Fig. 1(b). It can be noted that in order to approximate a beampattern with K points within a satisfactory MSE level, one would at least require antennas in the order of $\sqrt{K}$.

In the next series of examples, we conduct similar experiments for a different beampattern that has a slightly more complicated structure than in the first case. We consider a design scenario where the initial direction of arrival (DoA) information about $\tilde{K} = 3$ targets with unit complex amplitudes, approximately located at angles $\{-50°, 0°, 50°\}$ is available through a different method such as Capon or the GLRT method [14]. Hence, we design a symmetric beampattern with three points of interest $\tilde{\theta}_1 = -50°$, $\tilde{\theta}_2 = 0°$, and $\tilde{\theta}_3 = 50°$, respectively, and the beampattern of width $\triangle = 20°$:

$$d(\theta) = \begin{cases} 1, & \theta \in [\tilde{\theta}_k - \frac{\triangle}{2}, \tilde{\theta}_k + \frac{\triangle}{2}], \quad k = 1, 2, 3, \\ 0, & \text{otherwise} \end{cases} \tag{34}$$

as can be seen in in *black* in Fig. 2. It is clear from this figure that albeit the aforementioned beam is defined in 181 points similar to the previous case, it requires more number of antenna elements to be accurately realized due to its complex structure, which will be translated to higher first- and second-order resolutions.

Another example is considered in Fig. 3, where the desired beampattern has an impulse like shape (shown in *black*). The general structure of the beam follows a similar formulation as in (34), with the beampattern width $\triangle = 2°$. As expected, it is evident from Fig. 3 that an impulse-like beampattern with the same zero-order resolution as before requires even more antenna elements to be *accurately* realized.

V. Conclusion and Future Works

In this paper, we discussed the fundamental limitations of the resolution of beampatterns produced by MIMO radars in relation to their number of antennas. We provided multiple analytical results to show how the changes in a beampattern are impacted by an increased number of antennas in a massive MIMO scenario. As a future research avenue, we plan to discuss the characterization and efficient construction of such beampatterns.

References

[1] J. Li and P. Stoica, *MIMO Radar Signal Processing*, ser. Wiley - IEEE. Wiley, 2008.

[2] C. Zhang, Y. Huang, Y. Jing, and L. Yang, "Energy efficient beamforming for massive MIMO public channel," *IEEE Transactions on Vehicular Technology*, vol. 66, no. 11, pp. 10 595–10 600, 2017.

[3] S. Noh, M. D. Zoltowski, Y. Sung, and D. J. Love, "Pilot beam pattern design for channel estimation in massive MIMO systems," *IEEE Journal of Selected Topics in Signal Processing*, vol. 8, no. 5, pp. 787–801, 2014.

[4] T. L. Marzetta, "Noncooperative cellular wireless with unlimited numbers of base station antennas," *IEEE Transactions on Wireless Communications*, vol. 9, no. 11, pp. 3590–3600, 2010.

[5] B. L. Ng, Y. Kim, J. Lee, Y. Li, Y. Nam, J. Zhang, and K. Sayana, "Fulfilling the promise of massive MIMO with 2D active antenna array," in *2012 IEEE Globecom Workshops*, 2012, pp. 691–696.

[6] S. Fortunati, L. Sanguinetti, F. Gini, M. S. Greco, and B. Himed, "Massive MIMO radar for target detection," *IEEE Transactions on Signal Processing*, vol. 68, pp. 859–871, 2020.

[7] A. F. Molisch, V. V. Ratnam, S. Han, Z. Li, S. L. H. Nguyen, L. Li, and K. Haneda, "Hybrid beamforming for massive MIMO: A survey," *IEEE Communications Magazine*, vol. 55, no. 9, pp. 134–141, 2017.

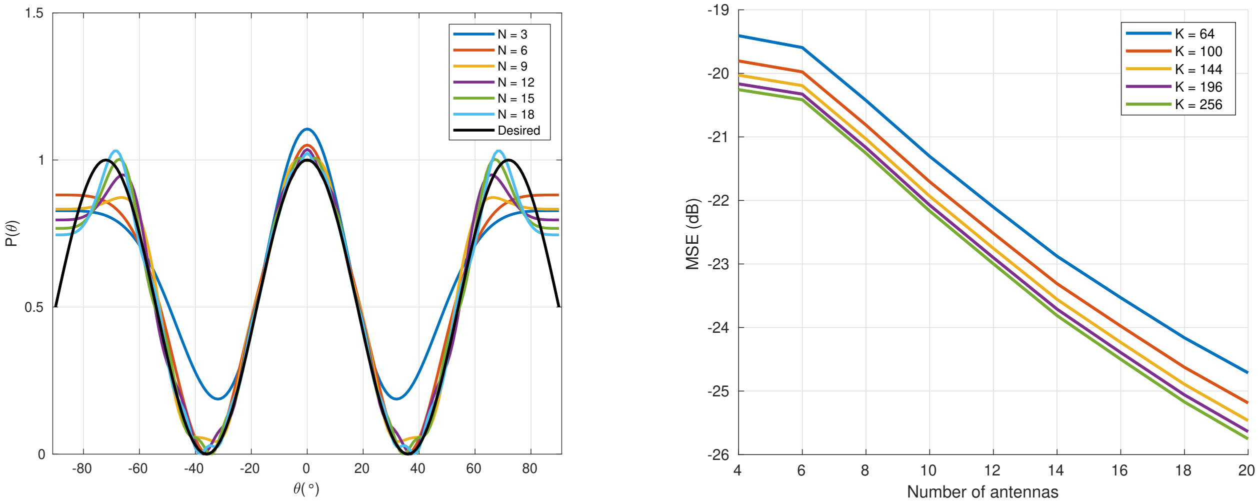

(a) (b)

Fig. 1. (a) Realization of a smooth sinusoidal beampattern with zero-order resolution $K = 181$ using $N \in \{3, 6, 9, 12, 15, 18\}$ antennas, (b) The mean square errors (MSE) of approximation of smooth beampatterns for different zero-order resolutions, $K \in \{64, 100, 144, 196, 256\}$, using $N \in \{4, 6, 8, 10, 12, 14, 16, 18, 20\}$ antennas.

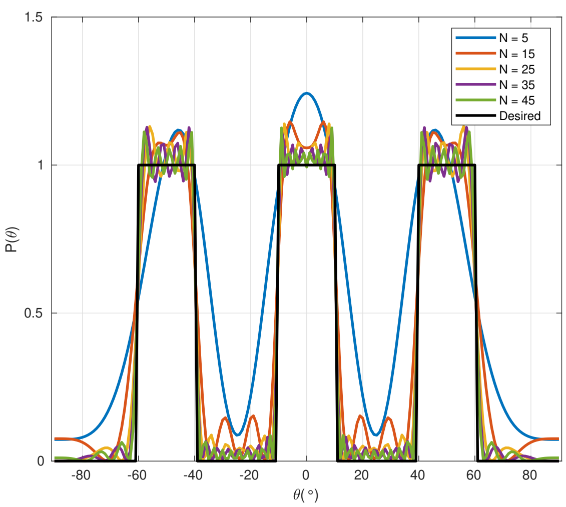

Fig. 2. Realization of a rectangular beampattern with resolution $K = 181$ using $N \in \{5, 15, 25, 35, 45\}$ antennas.

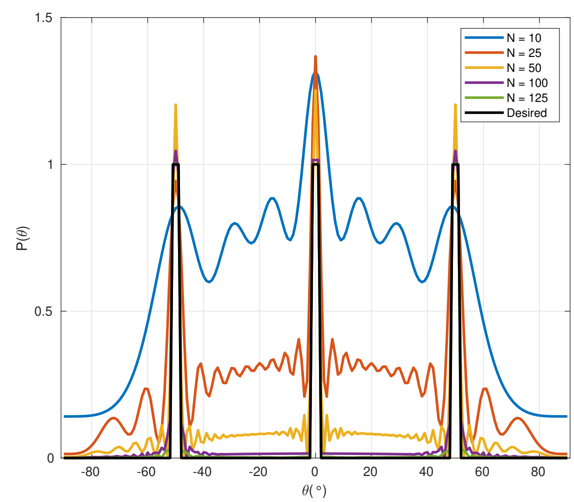

Fig. 3. Realization of a impulse-like beampattern with resolution $K = 181$ using $N \in \{10, 25, 50, 100, 125\}$ antennas.

[8] I. Selinis, K. Katsaros, M. Allayioti, S. Vahid, and R. Tafazolli, "The race to 5G era; LTE and Wi-Fi," *IEEE Access*, vol. 6, pp. 56 598–56 636, 2018.

[9] F.-C. Li, Y.-N. Zhao, P.-C. Gong, L. Feng, X.-K. Wan, and Y. Li, "Beamforming for hyperthermia treatment by training a weighted network of an ultrasonic array," *Health information science and systems*, vol. 5, no. 1, pp. 17–17, Dec 2017.

[10] A. Bose, S. Khobahi, and M. Soltanalian, "Joint optimization of waveform covariance matrix and antenna selection for MIMO radar," in *2019 53rd Asilomar Conference on Signals, Systems, and Computers*, 2019, pp. 1534–1538.

[11] M. Soltanalian, H. Hu, and P. Stoica, "Single-stage transmit beamforming design for mimo radar," *Signal Processing*, vol. 102, pp. 132–138, 2014.

[12] P. Stoica, R. L. Moses, and others, *Spectral analysis of signals*. Pearson Prentice Hall Upper Saddle River, NJ, 2005, ch. 6.

[13] M. Soltanalian and P. Stoica, "Computational design of sequences with good correlation properties," *IEEE Transactions on Signal processing*, vol. 60, no. 5, pp. 2180–2193, 2012.

[14] J. Li and P. Stoica, "MIMO radar with colocated antennas," *IEEE Signal Processing Magazine*, vol. 24, no. 5, pp. 106–114, 2007.

[15] P. Stoica, J. Li, and Y. Xie, "On probing signal design for MIMO radar," *IEEE Transactions on Signal Processing*, vol. 55, no. 8, pp. 4151–4161, 2007.

[16] A. Kalantari, M. Soltanalian, S. Maleki, S. Chatzinotas, and B. Ottersten, "Directional modulation via symbol-level precoding: A way to enhance security," *IEEE Journal of Selected Topics in Signal Processing*, vol. 10, no. 8, pp. 1478–1493, 2016.